Nigerian Journal of Technology (NIJOTECH)
Vol. 42, No. 2, June, 2023, pp.264 - 273
www.nijotech.com

Print ISSN: 0331-8443
Electronic ISSN: 2467-8821
https://doi.org/10.4314/njt.v42i2.15

ADAPTIVE REAL-TIME SPECTRUM SELECTION FRAMEWORK AND HANDOVER DECISION ALGORITHM (RSSF-HDA) FOR HETEROGENEOUS NETWORKS

V. O. Nkeleme[1,*], L. I. Oborkhale[2], and G. Sani[3]

[1,2] Department of Electrical/Electronic Engineering, Michael Okpara University of Agriculture Umudike, Abia State.
[3]Department of Computer Engineering, University of Calabar, Calabar, Cross River State, Nigeria

*corresponding author (Email: victornkeleme@gmail.com, Phone number: +234-806-569-4849)

Article history: Received 18 December, 2022. Revised 09 May, 2023. Accepted 26 May, 2023. Published 31 July, 2023.

Abstract
Carrier aggregation (CA) is a technology introduced by the Long-Term Evolution-Advanced (LTE-A) system to increase user throughput by combining a selected number of component carriers (CCs). Its integration with heterogeneous networks enables the mobile user equipment to take advantage of increased throughput and radio coverage of various access technologies. However, due to the mobility of user equipment, these innovations have increased the likelihood of handoff scenarios, resulting in a high outage probability and low throughput. Handover is a crucial part of mobility management since it enables users to move from one cell to another while maintaining connections. However, no single access technique can provide seamless communication without interruption or delay. As a result, creating a suitable handover decision algorithm is necessary for ensuring high-quality service continuity and dependable user equipment access to the network at all times. An Adaptive Real-Time Spectrum Selection Framework and Handover Decision Algorithm (RSSF-HDA) with optimal resource allocation to the deployed system model is presented in this paper. This effort is geared toward preventing communication failure and improving system performance. It further positions the 4G LTE-A framework for inclusive coexistence with the current 5G New Radio enhanced Mobile Broadband (eMBB) use case scenario. The results of the simulation reveal that this method increases system performance in terms of Cell edge spectral efficiency and Handover success rate above 10% and 13%, respectively, when compared to Conventional Handover Decision Algorithm (Conv-HDA) and Multi-Influence Factor Handover Decision Algorithms (MIF-HDA).

Keywords: Carrier Component, HetNet, handover, Carrier aggregation, CAD, Handover Algorithm.

1.0 INTRODUCTION
In wireless communication networks, several researchers have suggested various handover decision algorithms. During a conventional handover, prospective base stations' received signal strength (RSS) and/or power levels are compared [1]. Furthermore, other variables include (a) RSS with a threshold, (b) Hysteretic RSS, (c) RSS with hysteresis and threshold, (d) RSS with hysteresis and distance [2], (e) Signal-to-Interference-plus-Noise-Ratio (SINR) and (f) Interference-to-Interference-plus-Noise-Ratio (IINR) [1]. Nevertheless, their handover decision algorithms only take one parameter into account, while other contributing elements are not considered. As a result, non-intact handover decisions are made, which lowers a user's throughput and raises the likelihood of a call dropping. Consequently, the user and serving network's ability to communicate effectively is adversely affected. The Handover Decision Algorithm is based on several variables. However, additional influential variables have been neglected, such as interferences, noise, and resource availability. These significantly affect the efficiency of the system.

In recent times, there has been a surge in research and development aimed at expanding coverage and capacity to offer user equipment (UEs) an affordable greater data rate. As a result, there have been several innovative inventions, creative research endeavors, and significant evolutionary advancements in cellular networks [3][4]. Network efficiency is becoming more important as physical layer network advancements are made. Prior research has shown that systems based on robust Heterogeneous Networks (Het-Nets) design and greater utilization of radio spectrum via carrier aggregation methods are viable options [5] [6]. As a result, these two technology advancements serve as the foundation for network densification, with CA serving as an important capability included in the Third Generation Partnership Project (3GPP) Release 10 as a pivotal step towards Long Term Evolution Advanced (LTE-A) [1]. High data speeds and increased system capacity are anticipated to be supported by the addition of CA technology in LTE-A Release 10 (Rel.10) and later releases [6]. This indicates that an extremely desired aspect of LTE-A is the expansion of throughput.

LTE-A can aggregate up to five 20MHz CCs, each of which provides 100MHz capacity. As a result, data speeds as high as 1Gbps for downlink and 500Mbps for uplink are feasible [7]. While it is possible to aggregate only two or three CCs, Release 13 included support for CA up to 32 CCs, and Release 14 specified inter-band carrier aggregation up to five bands [8]. Furthermore, CA technology enables peak data throughput, backward compatibility, effective utilization of spectrum fragmentation, and the ability to support additional users with greater implementation efficiency [9] [10]. As a result, CA technology provides a solution for increased bandwidth demands and enables stable wireless connectivity suited for the future generation of communication networks. By employing contiguous and non-contiguous CA spectrum bands, CA provides a variety of deployment options for both homogeneous and heterogeneous networks.

A fundamental tool for mobile network operators (MNO) is flexibly combining CCs. The aggregate of two CCs from distinct bands is the primary focus of this work. This paper aims to develop an adaptive Real-time Spectrum Selection Framework and Handover Decision Algorithm (RSSF-HDA) with optimal resource allocation to the deployed system model on a standard LTE-Advanced system level uplink and downlink simulator—cell edge spectral efficiency and Handover success rate as reference key performance indicators.

1.1 Related Work

The study on LTE-A systems is limited since only a few studies have concentrated on system performance assessment based on different Carrier Aggregation Deployment Scenarios (CADS) [11]. However, researchers like [12] examined the performance improvements and complexity level that result from the combination of three inter-band 3CC as opposed to the combination of 2CC. Similarly, [9] investigated the handover event triggering time for intra-LTE mobility, and the impact of CA on mobility was assessed based on when the surrounding cells became offset better than the serving cell in terms of Reference Signal Received Power (RSRP) metrics. Table 1 shows the overview of CADS for LTE-A spectral enhancement [13].

Table 1: Overview of several CADS for LTE-A spectral efficiency enhancement [13]

CADS	Idea Base	Success	Limitations
CADS-1	-Contiguous band. -Equal coverage -Same Beam Direction (SBD)	-Provide equal RSRP over all the aggregated CCs. -Aggregate Contiguous Bands (ACB)	-High outage probability. - Low SE
CADS-2	-Non-contiguous band. -Overlapping coverage area. -SBD	-Aggregate Non-contiguous Bands (ANB)	-High outage probability -Low SE
CADS-3	-Non-contiguous band. -Co-located coverage area. -SBD	-Enhanced cell edge spectral efficiency of CC1 -ANB	Not Optimal
CADS-4	-Used RRH in a Noncontiguous band	-Enhanced cell edge spectral efficiency -Offload traffic from CC1	-High operation cost of deployment
CADS-5	-Non-Contiguous band. -Overlapping coverage area. -SBD	-Enhanced cell edge spectral efficiency of CC1 -ANB -Offload traffic	-Not optimal
CC-CADS	-Based on the contiguous band -Antenna beam directional from one CC to the boundary cell of the other -Equivalent coverage areas	-Enhanced cell edge spectral efficiency -Reduced outage probability	-Only single eNodeB Considered

Table 2: Truth Table

RSSI		PMTM		%MT > %RS	PCC		SCC		Target cell	
≥ TH_R	< TH_R	≥ TH_{RP}	< TH_{RP}		Serv	NoServ	Serv	NoServ	PCC	SCC
1	0	1	0	x	1	0	0	1	1	0
1	0	1	0	x	0	1	1	0	0	1
1	0	0	1	0	1	0	0	1	1	0
1	0	0	1	0	0	1	1	0	0	1
0	1	1	0	1	1	0	0	1	1	0
0	1	1	0	0	1	0	0	1	0	1
0	1	0	1	x	1	0	0	1	0	1
0	1	0	1	x	0	1	1	0	1	0
0	1	1	0	0	0	1	1	0	1	0
0	1	1	0	1	0	1	1	0	0	1

x – don't care; PMTM-Power Spectral Density using Multi-Tamper Method; PCC- Primary Component Carrier; SCC- Secondary Component Carrier; RSSI- Receive Signal Strength Indicator; TH_R – Threshold Value

[14] examined the handover and the decrease of UE's power consumption using the relaxation of Secondary Cells (SCell) measurement period of CADS in the cell's average throughput through the UE's mobility on two distinct CADS. [15] looked at the mobility performance for LTE Het-Nets with macro and Pico cells based on downlink inter-site CA. [16] assessed CADS #3-based challenges as well as traditional handover problem approaches. They also looked at cell spectral efficiency and UE throughput with respect to CADS #1 and #2. However, none of the researchers in the evaluated research sufficiently looked into the important handover performance metrics, including interruption duration, handover executed, call drops, and outage probabilities.

But [2] evaluated user mobility at various speeds to determine handover performance in coordinated contiguous CADS (CC-CADS). There are still issues with seamless handover performance in Het-Net settings. Hence contiguous band handover performance has not been completely investigated. The focus of this study will be on seamless and quick handover for LTE-A because it has remained a key design goal for the technology. As a result, in order to improve handover performance in CADS, this research develops a novel CADS known as the adaptive Real-time Spectrum Selection Framework and Handover Decision Algorithm (RSSF-HDA) by employing the Multi-Taper OFDMA Sensing of Reference Signal Received Power Estimator (MTO-RSRPE) technique.

2.0 PROPOSED HET-NETS CADS METHOD

This study proposes a feasible CA approach that utilizes two CCs in the same bands (Het-Nets CADS) using the Multi-Taper OFDMA Sensing of Reference Signal Received Power Estimator (MTO-RSRPE) technique implemented in an LTE-Advanced uplink and downlink system level simulator, as illustrated in Figure 1. This flowchart demonstrates the real-time spectrum selection framework by considering multivariate signals plus noise and matching each signal against the truth table (Table 2) and then applying Thompson multi-taper spectral estimation method upon a chosen window for averaging the PSD. As a result, the right signal is not only selected but also filtered for the target cell of the chosen CC. This approach is fast and appears in real-time, unlike the periodogram methods requiring widespread stationary processes.

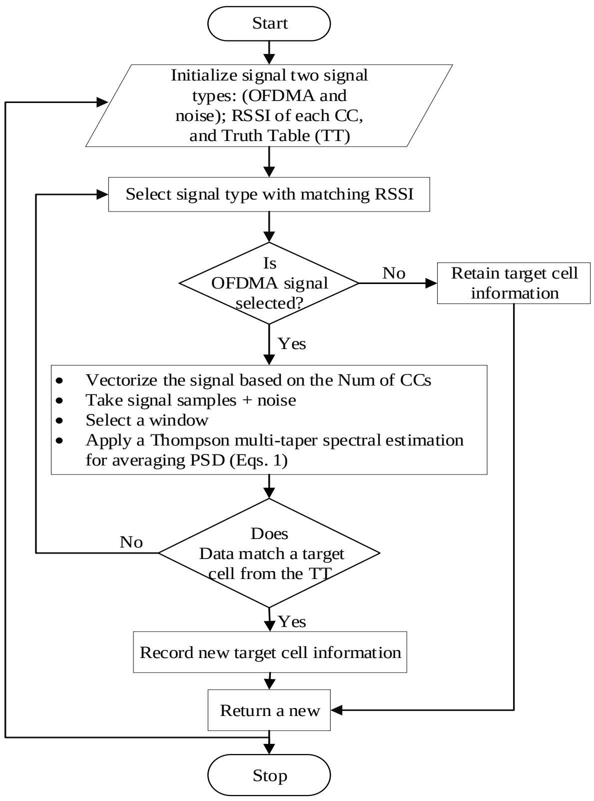

Figure 1: Flowchart of Multi-Taper OFDMA Sensing Algorithm

Additionally, the periodogram used to calculate a wide-sense stationary process for genuine power spectral density (PSD) is inconsistent. The multi-taper approach uses a set of mutually orthogonal windows or tapers to average modified periodograms in order to minimize the periodogram's variability. The tapers exhibit optimum time-frequency concentration characteristics in addition to mutual orthogonality. In order for this approach to work, the tapers' orthogonality, and time-frequency concentration are both essential. Thomson's multi-taper approach makes use of K-modified periodograms, each of which is created using a different Slepian sequence as the window, for spheroidal or sinusoidal signals, x(n), of discrete nature (containing a Slepian sequence) to achieve the following results:

$$S_k(n) = \delta t \left| \sum_{n=1}^{N-1} x(n) g_k(n)\, e^{-(i2\pi f n \delta t)} \right|^2 \qquad (1)$$

Where f is the frequency, δt is the difference with respect to time, and $g_k(n)$ is the k^{th} Slepian sequence.

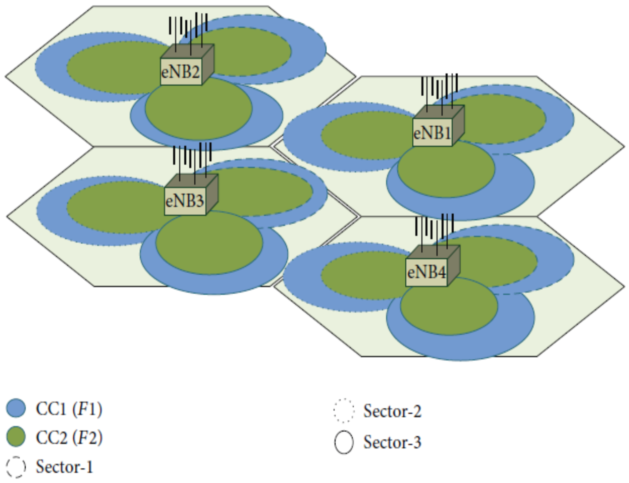

Figure 2: CAD with 3 sectors per eNodeB, with each having two contiguous CCs in the same antenna direction

In this wireless heterogeneous network with operating frequencies of 3.0 GHz and 3.6 GHz, there is an eNodeB positioned in the center of each cell, taking into account three (3) sectors within each cell. There is only one eNodeB, i.e., the one with primary CC (usually Macro), as shown in Figure 2. Secondary CC is an appendage drawn/hosted on the eNodeB in the form of a Microcell. Each sector was designed with two (2) contiguous Carrier Components (CCs). Each CC has an antenna that is oriented in a different direction towards one of the hexagonal cell's flat sides. To achieve the objective of a real-time spectrum selection framework, a global rendition algorithm was developed, upon which the novel (developed) RSSF-HDA program flowchart (Figure 3) was implemented. This algorithm is given in the next sub-heading.

2.1 RSSF-LTEA Global Rendition Algorithm

1. Initialize all *variables* and *rendition time loop =2000 seconds*
2. Allocate all resources according to *Table 3*
3. For each *UE_speed*
4. Build the LTEA network based on the deployment scenario
5. Allocate threshold values on *sinr*, *HOM*, and *TTT* according to *Table 3*
6. For each *rendition time loop t*
7. For each *eNodeB*
8. Generate sector-wise network traffic
9. End For (*eNodeB*)
10. Evaluate OFDMA signalization
11. For each *UE*
12. Implement Mobility Specification Algorithm
13. Obtain new UE vector positions and distance D from the serving eNodeB
14. For each *sector*
15. For each *CC*
16. Compute the directional gain G_{dB} from Equation (2)
17. Evaluate path loss $PathLoss_{dB}$ from Equation (3)
18. Estimate the received power from $P_r = P_{Tx} + G_{dB} + UE_{gain} - PathLoss + fast\ fading$
19. Evaluate $RSRP = 10^{\frac{P_r - 30}{10}}\ (dB)$
20. End For (*CC*)
21. End For (*sector*)
22. Implement RSSF–HDA according to the flowchart in *Fig. 3*
23. End For (*UE*)
24. End For (*rendition time loop*)
25. End For (*UE_speed*)

$$G_{dB} = 10 \log\left(G_t\, sinc\left(\frac{\phi - \psi}{s_r}\right) sinc\left(\frac{\phi - \psi}{s_r}\right)\right) \qquad (2)$$

Where $G_t = f(BW)$ is the transmitted gain, ϕ is the beam angle, ψ is the azimuth, and s_r is the scaling factor.

$$PathLoss_{dB} = 128.1 + 37.6\ log(D) + 21\ log\left(\frac{f_c}{2.0}\right) + normal\ shadowing \qquad (3)$$

From the global rendition algorithm, Step 1 initializes all variables, including the simulation time loop. In step 2, some resource allocation based on Table 3, necessary for building the deployed LTE-A Het-Nets scenario (step 4), is carried out. Other network resources, such as the threshold for the signal-to-interference-noise-ratio (sinr), handover margin (HOM), and time-to-trigger (TTT), are assigned in step 5. Models such as the sector-wise traffic generation (step 8), UE mobility (step 12), and the received power (RSRP) in step 19 are implemented for the respective eNodeB and each UE under the selected UE speed. Finally, RSSF-HDA is implemented in step 22, according to Figure 3.

2.2 Simulation Scenarios

The proposed algorithm is implemented as a Multicell system using MATLAB toolbox level simulator to generate LTE-A heterogeneous network Topologies. There are several built-in libraries and capabilities in MATLAB that can translate C and C++ code into MATLAB codes. Also, it enhances the potential of new technology and raises the security surrounding new technology. It also permits essential data modification [1]. MATLAB was employed as was used in earlier research [2]; [17]:[1].

The 3GPP LTE-A standard topology, 3GPP TS 36.211 version 10.3.0 Release 10 (2011), 3GPP TR 36.942 V11 (2012), and 3GPP TS 36.300 V11 (2012) were used to implement the network scenario setup by overlaying PiNodeBs over the MeNodeBs coverage area with a uniform user's distribution. The 61 hexagonal cells of macro eNodeB, which is centrally positioned and 500 meters apart from other sites, make up the simulated environment under consideration. In order to create the CCs in an inter-band non-contiguous deployment, the MeNodeBs are separated into three sectors, each of which is equipped with omnidirectional coverage Picocells. Based on the spectrum scenarios for Releases 13 and 14 (3GPP TR 36.942 V10.3.0,2012), the operational frequencies for CC1 and CC2 are 3.0GHz and 3.6GHz, respectively (3GPP TR 36.942 V10.3.0,2012).

MATLAB scripts (M-files) were developed for the proposed deployed system model for the sensing and Handover Deployment algorithm (HODA) with optimal resource allocation. The standard Vienna LTE-Advanced uplink and downlink system level simulator was used to implement the proposed spectrum sensing, component selection, and handover decision algorithms. This formed the basis for validation and performance comparison with other existing algorithms (MIF-HAD, Conventional (legacy) HDA) and collected data from MTN Network. The work also consists of the development of Source Codes (scripts) for MIF-HDA and Conv-HAD for use in the performance metrics comparison for the three algorithms.

Across the Picocell coverage region, the UEs are evenly dispersed. Consideration is given to Adaptive Modulation and Coding (AMC) methods as described in 3GPP's "TS 136 211 - V14.2.0, 2017". Under the assumption of 320ms as a time to trigger and 10dB as the handover margin, the handover process adheres to the protocols specified in (3GPP TS 36.33 1 version 10.20.0 Release 10, 2017). The simulation takes into account NaS processes, Radio Link Failure (RLF), and radio resource connection re-establishment in order to increase performance accuracy. It was crucial to implement the handover procedure described in 3GPP TS 36.300 V11 (2012). Based on the LTE-Advanced system profile specified by the 3GPP standards, the critical parameters utilized in the simulation are presented in Table 3.

In each Transmission Time Interval (TTI), 30 mobile UEs are randomly assigned to uniform locations in the serving and target cells. All through the design phase, which includes a range of mobile speed scenarios (3, 20, 30, 60, 100, and 130 km/h), the UEs' directional motions are to be chosen at random with a defined speed. All users' mobility movements must be taken into account within the first 32 cells, which are situated in close proximity to the center cell. For the duration of the simulation, each user will experience interference from six different eNodeBs, which are taken into account as the stations that produce these signals. The Frequency Reuse Factor (FRF) is considered to be 1. The Adaptive Modulation and Coding (AMC) scheme is also taken into consideration based on the sets of Modulation Schemes and Coding Rate that were established in [18] and [19].

Table 3: Resource allocation, Parameters, and Threshold Values

Allocation of Resources	
Number of eNodeB	61
Number sectors per eNodeB	3
Number of UE per cell	30
Cell Radius (R)in (m)	500
Number of Component Carriers (CC)	2
Carrier frequencies fc in (GHz)	[3.0, 3.6]
Bandwidth (BW) of each CC in (MHz)	20
Frequency Reused factor	1
Resource Block (RB) per CC	100
Subcarrier (SC) per RB	12
Symbols per subcarrier	7
BW per SC in (KHz)	15
Min Number of RBs per UEs	1
Max number of RBs per UEs	16
Slots per subframe	2
Subframe duration in (ms)	1
One slot duration in (ms)	0.5
RSSI	-101.50
Traffic Margin	10
All UE Speed in (km/hour)	[3 20 30 60 100 130]
Max Active UEs per CC	90
UE Parameters	
Max UE Tx power in (dBm)	23
Min UE Tx power in (dBm)	-40
Height in (m)	1.5
Number of MS antennas	1
Tx and Rx antenna gain in(dBi)	0
Noise figure in (dB)	9
eNodeB Parameters	
Tx Power in dBm	46
Antenna gain in (dBi)	15
Height in (m)	15
Noise figure (dB)	5
Log normal shadowing in (dB)	8
Modulation Constellation Size	
M_QPSK	4
M_16QAM	16
M_64QAM	64
Threshold values and HO Margin based on TS 36.331 V10.8.0, R2-092433, R2-093273	
sinr_QPSK_18 in (dB)	-6.5
sinr_QPSK_15 in (dB)	-4.2
sinr_QPSK_14 in (dB)	-3.5
sinr_QPSK_13 in (dB)	-1.5

sinr_QPSK_12 in (dB)	0.5
sinr_QPSK_23 in (dB)	2.0
sinr_QPSK_45 in (dB)	4.5
sinr_16QAM_12 in (dB)	6.1
sinr_16QAM_23 in (dB)	8.1
sinr_16QAM_45 in (dB)	10.9
sinr_64QAM_23 in (dB)	12.5
sinr_64QAM_34 in (dB)	15.5
sinr_64QAM_45 in (dB)	16.0
BER = 10^-3;	10^3
Min_HOM = 0	0
Max_HOM	10
Standard HOM = 0.5	0.5
Time-To-Triger (TTT) Thresholds based on TS 36.331 V10, R4-102114	
Min TTT in (ms)	0
Best TTT in (ms)	320
Max TTT in (ms)	5120
measurement interval in (ms)	40
Measurement factor	25
RCC Re-establishment Parameters based on TS 36.331	
T_311	10000
T_SI	80
T_PRACH	10
T_UL	30

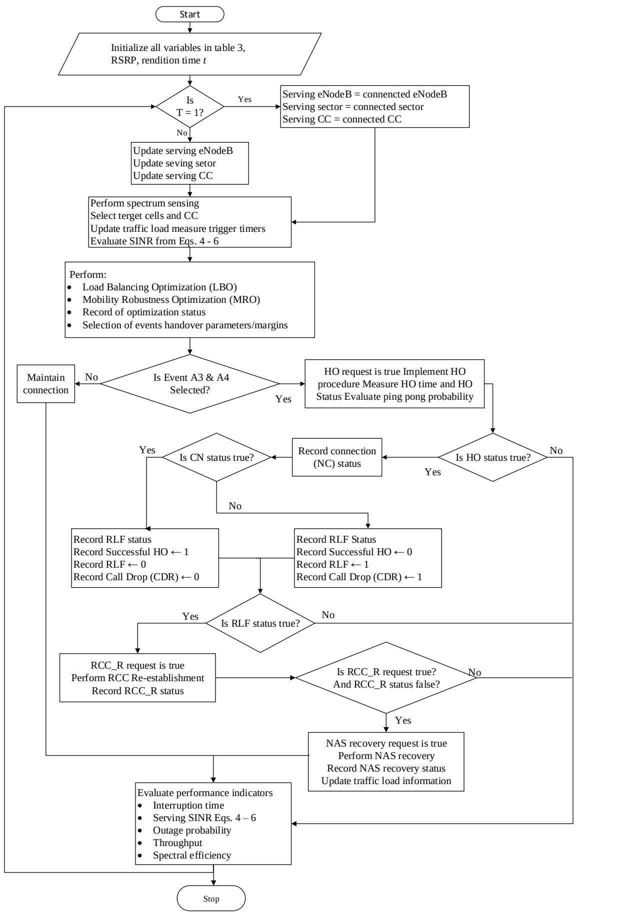

Figure 3: Flowchart of Proposed RSSF Handover Decision Algorithm

Event A3: Neighbour becomes the amount of offset better than serving;

Event A4: Neighbour becomes better than the absolute threshold;

$$P_n = 10\log(k * T_0) \quad (4)$$

$$\rho_N = 10^{\left(\frac{P_n + 10\log\left(BW * n * \frac{N_u}{N_{fft}}\right) + N_F}{10}\right)} \quad (5)$$

$$SINR = 10\log\left(\frac{10^{\frac{P_{rs}-30}{10}}}{\sum_{i=1}^{S_N} P_{ref_i} + \rho_N}\right) \quad (6)$$

Where k is Boltzmann's constant; T_0 is the temperature; BW is the bandwidth; n is the sampling factor, N_{fft} is the number of subcarriers; N_u is the number of used subcarriers; N_F is the noise figure; P_{rs} is the serving reference power; P_{ref} is the sectorized neighboring reference received power from sectors $i = 1,2, \ldots S_N$

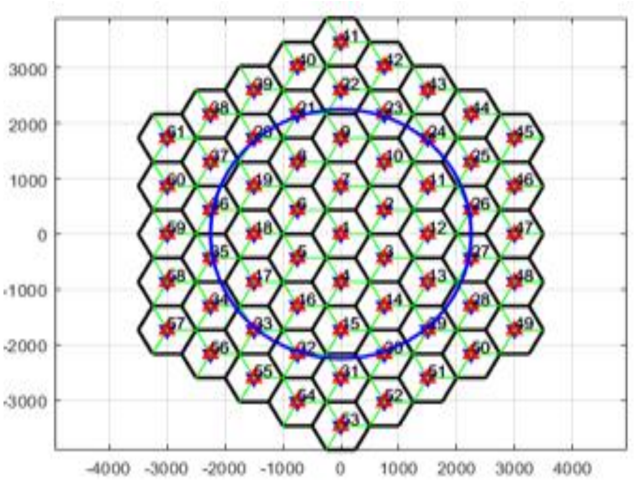

Figure 4: A view of the clustered eNodeBs in the deployment scenario

3.0 SIMULATION RESULTS

Results of the baseline Conventional Handover Decision Algorithm (Conv-HDA), Multi-Influence Factor Handover Decision Algorithms (MIF-HDA) performance, and the Proposed RSSF-HDA are shown in this section. Based on the use of hard handover at various mobile speeds, the outcomes were examined for the Outage probability, Cell edge spectral efficiency, Handover success rate, and System throughput. Thus, the Het-Nets CADS topology is shown in Figure 3. The topological design demonstrates that carrier aggregation allows for the deployment of additional UEs in macro and microcells. A total number of sixty-one (61) eNodeB are considered, with each eNodeB surrounded by six (6) neighbors. Thus seven (7) eNodeBs form one cluster, as shown in Figure 4. Additionally, each eNodeB is divided into three (3) sectors and covers an estimated radial distance (R) of five hundred meters (500m). finally, the mobility area of the mobile stations or User Equipment (UEs) has been defined (in blue circle) to a radius of about 5R.

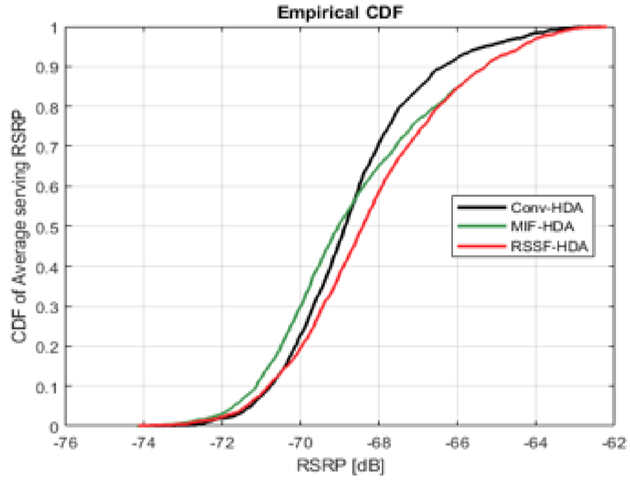

Figure 5: CDF probability of UE's RSRP over the serving RSRP

Results from Figure 5 show a plot of the CDF probability of the UE's RSRP (Y-axis) versus the serving RSRP (X-axis), indicating the performance of RSSF-HDA and the other methods (Conv-HDA and MIF-HDA). When compared to Conv-HDA and MIF-HDA, it is shown that RSSF-HDA offers a greater RSRP over the PCC it serves.

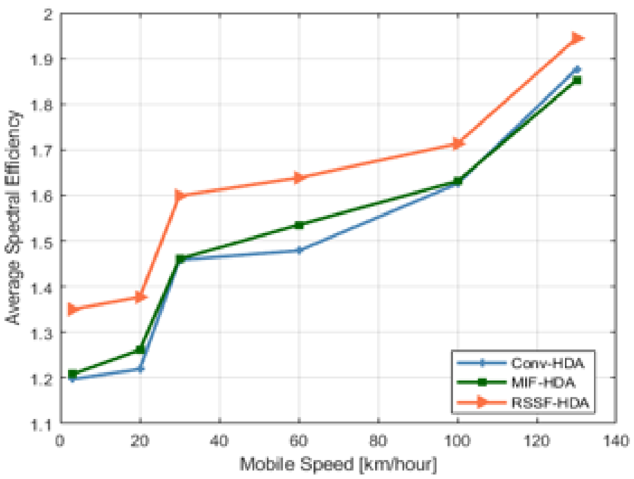

Figure 6: UE's Average spectral efficiency over all the mobile speeds

Figure 6 compares the average SE of the UE at various mobile speeds using the deployed RSSF-HDA, and the results are shown. The performance of the suggested RSSF-HDA in comparison to the other Handover algorithm can be seen in the plot of the mobile speed (x-axis) versus the SE (y-axis). The proposed RSSF-HDA performs better than the alternative Handover Decision Algorithm (HODA), as shown by the plot of the SE (y-axis) versus the mobile speed (x-axis). Generally, it appears from the results (Figure 6) that the average SE rises as UE speed rises. The outcomes shown in Figure 6 further imply that the proposed RSSF-HDA surpasses its counterparts for the speed under consideration. RSSF-HDA significantly outperforms the other HODAs in improving the average SE.

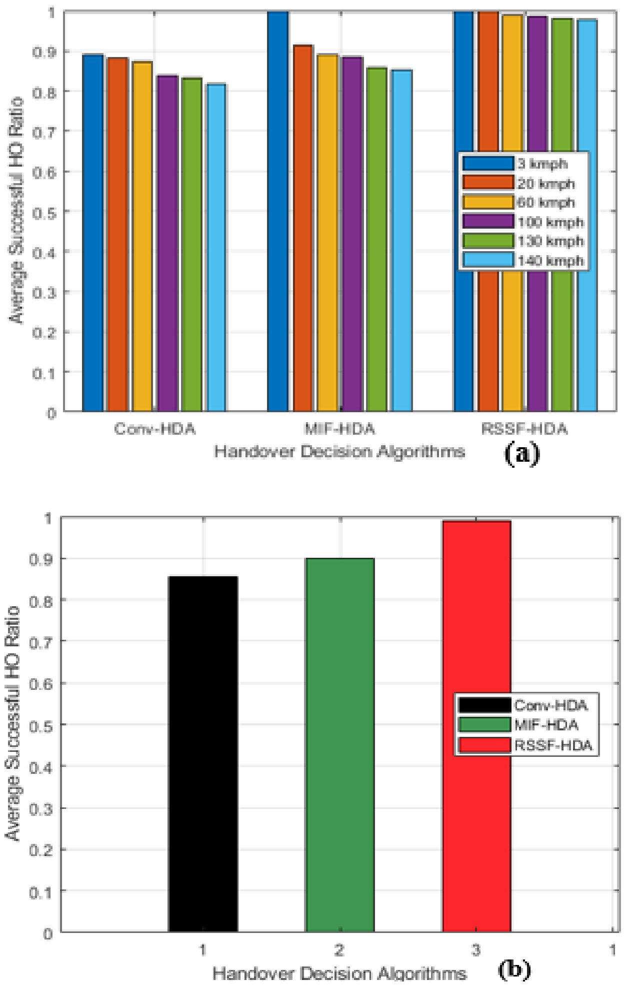

Figure 7: Successful Handover; (a) Average Successful Handover Ratio over All various speeds (b) Average Successful Handover Ratio over All Handover Decision Algorithm.

The signal handover successful ratio must also be taken into account while examining spectral efficiency. In Figure 6, the average handover success ratio is analyzed, and the findings show that it varies depending on the algorithm and the speed (see Figure 7). Contrary to spectrum efficiency, the average handover successful ratio gradually decreases as UE speed rises (Figure 7a). Results from Figure 7 further demonstrate how HODA has an impact on each average handover successful ratio at different speeds. In contrast to the other algorithms, which have 90%

for MIF-HDA and 86% for Conv-HDA average handover success rates at 60 kmph, RSSF-HDA has a 98% average handover successful ratio at this speed.

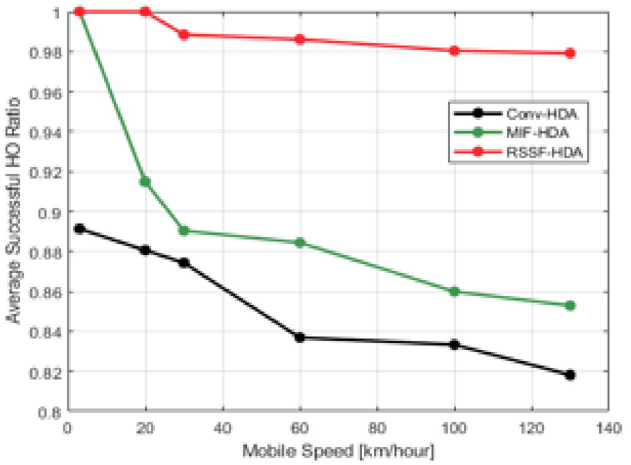

Figure 8: Average Successful Handover Ratio over All Mobile Speed

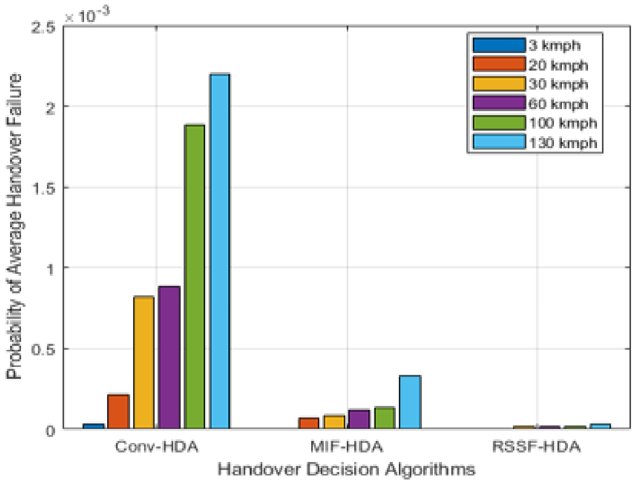

Figure 9: Probability of Average Handover Failure over Handover Decision Algorithm

Nevertheless, at the highest speed (140 kmph) examined in the simulation, RSSF-HDA has an average handover successful ratio of 96%, whereas Conv-HDA and MIF-HDA have 82% and 86%, respectively. In addition, Figure 7's findings show that when compared to Conv-HDA and MIF-HDA, the RSSF-HDA showed a notable improvement in the average handover successful ratio. According to Figure 7b's performance of handover successful ratio compared to the other HODA findings, RSSF-HDA performs better on average than the others in terms of handover successful ratio. In comparison to MIF-HDA and Conv-HDA, for instance, RSSF-HDA experiences average improvement of 10% and 13%, respectively. Following that, Figure 9 shows the probability of handover failure for each scenario at various handover algorithms. When compared to MIF-HDA and Conv-HDA, RSSF-HDA has a significantly lower average handover failure overall speed. Figure 10 gives a clearer illustration of the variations among the considered Handover decision algorithms.

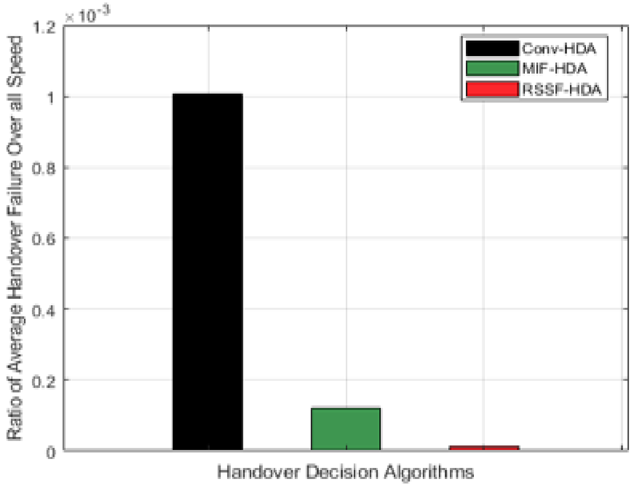

Figure 10: Probability of Average Handover Failure Overall Speed against Handover Decision Algorithms

4.0 CONCLUSION

In this work, a new handover decision algorithm known as RSSF-HDA was proposed. The proposed RSSF-HDA for an LTE-A system's handover performance was compared to that of two other HODA (MIF-HDA and Conv-HDA). The simulation analysis's findings show that RSSF-HDA may be more efficient in enabling wider bandwidth and greater SE than the existing HODA deployment. In comparison to other HODA taken into consideration in the research, RSSF-HDA SE has higher metrics, increasing from 1.35 bps/Hz/cell at mobile speeds of 20 kmph to 1.87 bps/Hz/cell at 120 kmph. Moreover, the use of RSSF-HDA based on spectrum sensing decreases the probability of outages, call drops, and handover ping-pong, which improves system performance.

Further advantages include improved end-user throughput, quicker inter-eNodeB load balancing, and mobility robustness when RSSF-HDA is implemented. In addition, results from the simulation demonstrated that, when compared to other HODA, RSSF-HDA maintains the probability of encountering handover failure and handover ping-pong at an acceptable minimal level. The efficiency, in this case, is credited to the availability of transmission bandwidth via intra-band contiguous CC mapping, as well as the effective joint proportional fair load balancing scheduling via spectrum sensing allocating UEs to the appropriate cell. Therefore, it is obvious that the use of spectrum sensing results in high SE gain across the cell at different speeds since it enables UEs to be allocated to the best channel regardless of modifications in the channel condition. Finally, further research can adopt this concept when adopting more carrier components. Finally, by introducing more carrier components, further research can use this approach.

REFERENCES

[1] Abdulazeez-Ahmed, M., Nordin, N. K., Sali, A. B., and Hashim, F. "Multi-criteria handover decision for heterogeneous networks: Carrier aggregation deployment scenario", *Int. J. Comput. Networks Commun.*, vol. 12, no. 4, pp. 41–54, Jul. 2020, doi: 10.5121/IJCNC.2020.12403.

[2] Shayea, I., Ismail, M., Nordin, R., and Mohamad, H. "Adaptive handover decision algorithm based on multi-influence factors through carrier aggregation implementation in LTE-advanced system", *J. Comput. Networks Commun.*, vol. 2014, 2014, doi: 10.1155/2014/739504.

[3] Qamar, F., Siddiqui, M. U. A., Hindia, M. H. D. A., Hassan, R., and Nguyen, Q. N. "Issues, Challenges, and Research Trends in Spectrum Management: A Comprehensive Overview and New Vision for Designing 6G Networks," *Electron. 2020, Vol. 9, Page 1416*, vol. 9, no. 9, p. 1416, Sep. 2020, doi: 10.3390/ELECTRONICS9091416.

[4] Siddiqui, M. U. A., Qamar, F., Tayyab, M., Hindia, M. H. D. N., Nguyen, Q. N., and Hassan, R. "Mobility Management Issues and Solutions in 5G-and-Beyond Networks: A Comprehensive Review", *Electron. 2022, Vol. 11, Page 1366*, vol. 11, no. 9, p. 1366, Apr. 2022, doi: 10.3390/ELECTRONICS11091366.

[5] Ibrahim, S. K., and Khamiss, N. N. "Optimization a Scheduling Algorithm of CA in LTE ADV", *TELKOMNIKA Telecommunication Comput. Electron. Control.*, vol. 16, no. 6, pp. 2514–2521, Dec. 2018, doi: 10.12928/TELKOMNIKA.V16I6.1 0054.

[6] Simarmata, R. F., Fahmi, A., and Meylani, L. "Analisis Kinerja Teknik Carrier Aggregation Tdd-fdd Di Lte-advanced Dengan Skenario Inter-band Carrier Aggregation", *eProceedings Eng.*, vol. 7, no. 2, Aug. 2020, Accessed: Dec. 06, 2022. [Online]. Available: https://openlibrarypublications.telkomuniversity.ac.id/index.php/engineering/article/view/12693

[7] "LTE; Requirements for further advancements for Evolved Universal Terrestrial Radio Access (E-UTRA) (LTE-Advanced)", 2010, Accessed: Dec. 07, 2022. [Online]. Available: http://portal.etsi.org/chaircor/ETSI_support.asp

[8] TSGR, "TS 136 101 - V13.2.1 - LTE; Evolved Universal Terrestrial Radio Access (E-UTRA); User Equipment (UE) radio transmission and reception (3GPP TS 36.101 version 13.2.1 Release 13)", 2016, Accessed: Dec. 06, 2022. [Online]. Available: https://portal.etsi.org/TB/ETSIDeliverableStatus.aspx

[9] Galih, R. "Carrier Aggregation Technique to Improve Capacity in LTE-Advanced Network", *TELKOMNIKA*, vol. 14, no. 1, pp. 1693–6930, 2016, doi: 10.12928/TELKOMNIKA.v14i1.2668.

[10] Wahidin, H. Putri, and Christiary, Y. "The Evaluation of the Throughput Performance of an LTE-Advanced Urban Area Network with the Inter-Band Non-Contiguous Carrier Aggregation Method", *J. Hunan Univ. Nat. Sci.*, vol. 49, no. 8, pp. 209–217, Aug. 2022, doi: 10.55463/ISSN.1674-2974.49.8.25.

[11] Zhang, R. "Radio Resource Management in LTE-Advanced Systems with Carrier Aggregation", Jun. 2016, Accessed: Dec. 06, 2022. [Online]. Available: https://uwspace.uwaterloo.ca/handle/10012/10552

[12] Qu, W., Fu, Y., and Zhao, Y. "A novel UE preference based component carrier selection algorithm in LTE-advanced", *IEEE Veh. Technol. Conf.*, vol. 2017-September, pp. 1–5, Feb. 2018, doi: 10.1109/VTCFALL.2017.8288060.

[13] "(PDF) Evaluation of Handover Performance on Heterogeneous Networks: Carrier Aggregation Deployment Scenarios with Femtocells", https://www.researchgate.net/publication/342638332_Evaluation_of_Handover_Performance_on_Heterogeneous_Networks_Carrier_Aggregation_Deployment_Scenarios_with_Femtocells (accessed Dec. 07, 2022).

[14] Shayea, I., Ismail, M., Nordin, R., Mohamad, H, Abd Rahman, T., and Abdullah, N. F. "Novel handover optimization with a coordinated contiguous carrier aggregation deployment scenario in LTE-Advanced systems", *Mob. Inf. Syst.*, vol. 2016, 2016, doi: 10.1155/2016/4939872.

[15] Karandikar, A., Akhtar, N., and Mehta, M. "Mobility Management in LTE Networks", *Mobil. Manag. LTE Heterog. Networks*, pp. 13–32, 2017, doi: 10.1007/978-981-10-4355-0_2.

[16] Tayyab, M., Gelabert, X., and Jantti, R. "A Survey on Handover Management: From LTE to NR", *IEEE Access*, vol. 7, pp. 118907–118930, 2019, doi: 10.1109/ACCESS.2019.2937405.

[17] Maaloul, S., Afif, M., and Tabbane, S. "Handover Decision in Heterogeneous Networks", in *2016 IEEE 30th International Conference on Advanced Information Networking and Applications (AINA)*, Mar. 2016, pp. 588–595. doi: 10.1109/AINA.2016.33.

[18] TSGR, "TS 136 211 - V10.3.0 - LTE; Evolved Universal Terrestrial Radio Access (E-UTRA); Physical channels and modulation (3GPP TS 36.211 version 10.3.0 Release 10)", 2011, Accessed: Dec. 11, 2022. [Online]. Available: http://portal.etsi.org/chaircor/ETSI_support.asp

[19] Arib, "3rd Generation Partnership Project; Technical Specification Group Radio Access Network; Evolved Universal Terrestrial Radio Access (E-UTRA); TDD Home eNode B (HeNB) Radio Frequency (RF) requirements analysis (Release 11)", 2012, Accessed: Dec. 06, 2022. [Online]. Available: http://www.3gpp.org